JPNT 8(3), 119-127 (2019)
https://doi.org/10.11003/JPNT.2019.8.3.119

JPNT Journal of Positioning, Navigation, and Timing

Assessment on the Performance of Search And Rescue Service of KPS

Jung-Hoon Lee[1], Sanguk Lee[2], Jong-Hoon Won[1†]

[1]Department of Electrical Engineering, Inha University, Incheon 22212, Korea
[2]Radio Satellite Research Div., ETRI, Daejeon 34129, Korea

ABSTRACT

COsmicheskaya Sisteyama Poiska Avariynich Sudov Search and Rescue Satellite-Aided Tracking (COSPAS-SARSAT) is an international communication support program to perform search and rescue (SAR) operations in emergency situations by using satellite signals relayed from a beacon. The legacy COSPAS-SARSAT was originally composed of low altitude and geostationary Earth orbit satellites; thus, a limited number of directional dish antennas was sufficient to cover the limited number of visible satellites at the local user terminal. However, the second generation COSPAS-SARSAT newly added the medium Earth orbit satellites, e.g., Global Navigation Satellite Systems (GNSS) to the existing system, so that the number of visible satellites increase dramatically, and the system upgrade to cover all the visible satellites is foreseen. The additional use of planned Korea Positioning System (KPS) to existing GNSS is envisaged to provide a better performance of their SAR service. This paper presents the benefits of the additional use of KPS together with the phased array antennas at the local user terminal of the COSPAS-SARSAT. This is to effectively response to the increase of the number of visible satellites. Numerical simulation is included to evaluate the performance improvement of COSPAS-SARSAT in terms of the number of visible satellites, geometry between satellites and user, and position estimation accuracy.

Keywords: COSPAS-SARSAT, joint dilution of precision, MEOSAR, KPS

1. INTRODUCTION

COsmicheskaya Sisteyama Poiska Avariynich Sudov Search and Rescue Satellite-Aided Tracking (COSPAS-SARSAT) is an international disaster relief communication support program, in which people, aircraft, ships, and so on in emergency situations activate the 406 MHz beacon and send search and rescue signals to national emergency rescue agencies.

Fig. 1 shows an overview of the COSPAS-SARSAT system consisting of beacons to transmit the coded data burst of the rescue signal, satellites for rescue signal relay, a local user terminal (LUT), that is, a ground station to undertake reception and signal processing, a mission control center

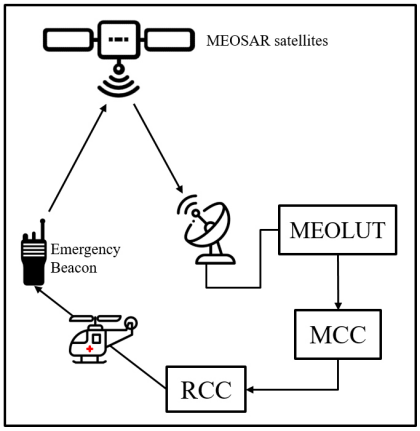

Fig. 1. COSPAS-SARSAT system overview.

Received Jul 03, 2019 **Revised** Aug 16, 2019 **Accepted** Aug 26, 2019
†**Corresponding Author**
E-mail: jh.won@inha.ac.kr
Tel: +82-32-860-7406 Fax: +82-32-863-5822
Jung-Hoon Lee https://orcid.org/0000-0002-0875-016X
Sanguk Lee https://orcid.org/0000-0002-0744-5032
Jong-Hoon Won https://orcid.org/0000-0001-5258-574X

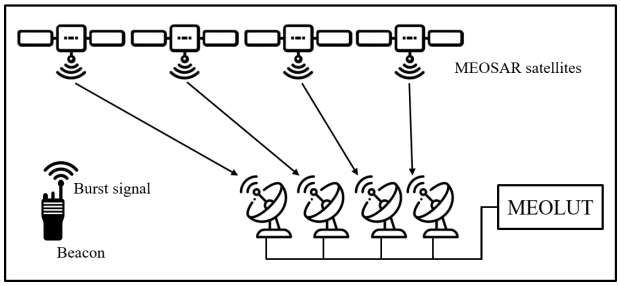

Fig. 2. MEOLUT system with directional dish antenna.

(MCC) to distribute rescue data to rescue centers, and a rescue coordination center (RCC) (COSPAS-SARSAT 2018a).

The legacy COSPAS-SARSAT used Low Earth Orbit Search and Rescue (LEOSAR) and Geostationary Earth Orbit Search and Rescue (GEOSAR). GEOSAR can cover the entire earth except the polar regions, but cannot use the Doppler effect effectively because geostationary satellites have relatively small movement between the distress beacon and the satellites. Comparatively, LEOSAR satellites can use the Doppler effect efficiently, but its relatively low altitude makes it impossible to cover the entire earth in real time. Therefore, Medium Earth Orbit Search and Rescue (MEOSAR), that is to use Medium Earth Orbit satellites, such as Global Navigation Satellite System (GNSS) satellites, is being promoted to overcome the drawbacks of satellites at low or geostationary earth orbit. MEOSAR can cover the entire earth in real time and can also use the Doppler effect effectively (COSPAS-SARSAT 2018a).

The message protocol of the 406 MHz COSPAS-SARSAT beacons contains the location information obtained by a GNSS receiver equipped in the beacon. Therefore, it is possible to estimate the position of the beacon even by decoding the signal without additional technology. However, if the GNSS receiver equipped in the beacon is faulty or unusable for any reason, the beacon location must be estimated using only beacon signals relayed by multiple satellites (COSPAS-SARSAT 2018b). This paper assumes this fault situation exists. Thus, the estimated location from any navigation devices equipped in the beacon is not usable. This means that the Medium-altitude Earth Orbit Local User Terminal (MEOLUT) should estimate the beacon's location using only the received beacon signals.

Meanwhile, the conventional COSPAS-SARSAT LUT antenna is shown in Fig. 2. In the past when only GEOSAR and LEOSAR were used, the number of COSPAS-SARSAT visible satellites was limited. A directional dish antenna is configured to track only one satellite at a high gain to reduce interference with other satellite signals. Thus, multiple directional dish antennas are required to receive multiple satellite signals at one LUT. For a stand-alone LUT, 4 to 6 antennas are considered sufficient (for economic reasons) to cover the visible satellites. To increase the number of visible satellites, the LUTs are connected to each other via a network, and share the received data to enhance the position estimation ability (COSPAS-SARSAT 2018c).

The use of MEOSAR, which is currently in operation, will increase the number of visible satellites dramatically in comparison to LEOSAR or GEOSAR due to its medium Earth orbit constellation. Recent developments in electronic and communication technologies, and economic reasons have made all-in-view processing using a phased array antenna at LUTs feasible. Therefore, MEOLUT tends to upgrade its directional dish antennas to phased-array antennas. Recently, MEOLUT in France was upgraded with the phased array antenna to track up to 30 satellites, simultaneously (Martin et al. 2018). Therefore, when estimating the position using time difference of arrival (TDOA) and frequency difference of arrival (FDOA) by the all-in-view method, it is necessary to analyze the change in dilution of precision (DOP) of COSPAS-SARSAT and the resulting location estimation accuracy.

Because COSPAS-SARSAT is a disaster relief communication support program, accurate location estimation of a beacon is obviously important. A preliminary result on the use of the block adjustment of synchronizing signal algorithm to increase the estimation performance of signal processing in the COSPAS-SARSAT system was presented and analyzed in terms of various signal environments as well as a receiver parameter (e.g., sampling rate) (Lee et al. 2018).

In addition, for accurate position estimation, the number and arrangement of visible satellites that are seen together at the beacon and LUTs at the same time are key factors. When satellites are used for navigation, the arrangement of satellites directly affects the positioning accuracy. DOP is a measure of the quality for the geometrical arrangement of visible satellites. In comparison to GNSS that uses time of arrival (TOA) and frequency of arrival (FOA) for position estimation, COSPAS-SARSAT uses TDOA and FDOA for position estimation. The DOP formula has been newly defined to determine the quality of the geometrical arrangement of COSPAS-SARSAT satellites (Paiement et al. 2008).

Meanwhile, developments to the Korea Positioning System (KPS) are currently under discussion (GPS World 2018). According to the development plan, it will be launched by 2034, providing positioning and timing services over an area spanning a 1000 km radius from the

country's capital, Seoul. In order to provide the planed service performance, one of the candidate plans for the proposed KPS constellation is to have a total of seven satellites consisting of three geostationary satellites and four Inclined-Geosynchronous-Orbit (IGSO) satellites. One of the envisaged services of the KPS is Search And Rescue (SAR) service as same to some other GNSS. A modeling and simulation tool for the distress beacon of KPS was developed to analyze the accuracy, reliability, and availability of the SAR system (Jeong et al. 2019). The use of KPS together with the existing MEOSAR will provide a positive synergic effect in the Korean peninsula region on the number of visible satellites, DOP, and position estimation performance. Therefore, the relevant analysis is needed.

The remainder of this paper is organized as follows. First, we briefly describe the COSPAS-SARSAT system model. Then, we present the numerical simulation results to analyze the benefit of the use of phased array antennas in comparison to the use of directional dish antennas in terms of the number of visible satellites, DOP and position accuracy. The additional benefits obtained by the use of KPS is also discussed. And, finally, we conclude by outlining the distinctive benefits of our approach.

2. COSPAS–SARSAT SYSTEM MODEL

2.1 Signal Structure

The signal model used in this paper is based on a second-generation 406 MHz beacon. In February 2018, COSPAS-SARSAT newly updated the second-generation beacon signal. The second-generation beacon signal was modulated with direct-sequence-spread-spectrum offset-quadrature-phase-shift-keying (DSSS-OQPSK). The length of the signal is fixed at 1 s, and the coded data burst is transmitted every 5 s. The pseudorandom number (PRN) is generated using the shift register, where the total code length is 38,400 chips. The data rate is 300 bps, so that the signal carries a total of 300 bits. The initial 50 bits of the signal is a preamble message, and all signals are the same. Among the remaining 250 bits, 202 bits are useful messages and 48 bits are error correction codes. The error correction code uses BCH (250,202), that is, the shortened form of BCH (255,207) (COSPAS-SARSAT 2018d).

In this study, we use PRN codes in normal mode, and 202 bits of data are randomly generated. The 48-bit error correction codes are generated using 202-bit useful messages. After generating the beacon signal, TOA and FOA of the selected satellites are calculated, and the received signal is generated according to each TOA, FOA, and C/N_0.

2.2 Signal Processing

MEOLUT estimates the TOA and FOA of the beacon signal, and uses the result to find the beacon location (COSPAS-SARSAT 2018c). In this signal processing, the TOA and FOA of the signal are estimated using the cross-ambiguity-function (CAF), that is, a function to calculate the similarity of the two signals through correlation processing (Hartwell 2005).

$$CAF(\tau, f) = \int_0^T s_r(t) s_l^*(t+\tau) e^{-(j2\pi f t)} dt \tag{1}$$

where,

s_r: received input signal
s_l: locally-generated signal
τ: time lag parameter [s]
f: frequency offset parameter [Hz]
T: integration time [s]

The basic method of calculating CAF is a summation, which finds the peak value after calculations in all time and frequency cells. However, with this method, the computational complexity increases rapidly depending on the range of time and frequency. Therefore, Fast-Fourier-Transform (FFT) method or Fast-Fourier-Transform and Inverse-Fast-Fourier-Transform (FFT-IFFT) method is used in order to reduce the computational complexity. We use the FFT-IFFT method to estimate the TOA and FOA.

The equations for TOA and FOA using the FFT-IFFT method are as follows (Tsui 2005).

$$v(n) = \sum_{m=0}^{N-1} s_r(m) s_l(n+m) \tag{2}$$

$$V(k) = \left[\sum_{m=0}^{N-1} s_r(m) e^{j2\pi \frac{km}{N}}\right]\left[\sum_{n=0}^{N-1} s_l(n+m)\, e^{-j2\pi \frac{k(n+m)}{N}}\right] \tag{3}$$

$$V(k) = S_l^{-1}(k) S_r(k) \tag{4}$$

$$|V(k)| = |S_l(k) S_r^*(k)| \tag{5}$$

where,

N: the number of samples

From the input signal and locally-generated signal which is at the center frequency of the i-th index, the $|V_i(k)|$ is

calculated, and then, transformed into $|v_i(n)|$ using the IFFT. The peak of $|v_i(n)|$ in time domain index n and frequency domain index i indicate TOA and FOA.

2.3 Localization Method

COSPAS-SARSAT estimates the beacon location using a combination of TDOA and FDOA. MEOLUT measures the TOA and FOA of each signal, and uses these measurements to calculate TDOA and FDOA for 2- or 3-dimensional locations (COSPAS-SARSAT 2018c). The equations for TDOA and FDOA are as follows (Hartwell 2005):

$$TDOA_{ba} = \frac{1}{c}\left(\sqrt{(x_b - x)^2 + (y_b - y)^2 + (z_b - z)^2} - \sqrt{(x_a - x)^2 + (y_a - y)^2 + (z_a - z)^2}\right) \quad (6)$$

$$FDOA_{ba} = \frac{f_c}{c}\left(\frac{v_{x,b}(x_b - x) + v_{y,b}(y_b - y) + v_{z,b}(z_b - z)}{\sqrt{(x_b - x)^2 + (y_b - y)^2 + (z_b - z)^2}} - \frac{v_{x,a}(x_a - x) + v_{y,a}(y_a - y) + v_{z,a}(z_a - z)}{\sqrt{(x_a - x)^2 + (y_a - y)^2 + (z_a - z)^2}}\right) \quad (7)$$

where,

c: speed of light
f_c: carrier frequency
x,y,z: emitter (i.e., beacon) position
x_a, y_a, z_a: position of collector A
x_b, y_b, z_b: position of collector B
v_{xa}, v_{ya}, v_{za}: relative velocity of collector A and emitter
v_{xb}, v_{yb}, v_{zb}: relative velocity of collector B and emitter

In order to estimate the 3-dimensional position, at least three TDOA or FDOA measurements are necessary, which is equivalent to the fact that at least four received signals are required to solve navigation equations. Since the equations of TDOA and FDOA are non-linear, nonlinear least-square estimation (NLSE) should be used to obtain solution. This is done by linearizing the value for estimating the function and iteratively calculating the estimate using the linearized measurement value (Hartwell 2005).

$$F(\underline{x}) = F(\underline{x}_0) + \frac{\partial}{\partial \underline{x}} F(\underline{x}_0)\delta\underline{x} + h.o.t \quad (8)$$

where,

$\delta\underline{x}$: $\underline{x}$ - x_0
$\underline{x}_0$: nominal state vector
$h.o.t$: high order terms

The first-order differential matrix of TDOA is as follows:

$$R_i = \sqrt{(x_i - x)^2 + (y_i - y)^2 + (z_i - z)^2} \quad (9)$$

$$\frac{\partial(TDOA_{i1})}{\partial x} = \frac{(x - x_i)}{R_i} - \frac{(x - x_1)}{R_1} \quad (10)$$

$$H_{TDOA} = \begin{bmatrix} \frac{\partial(TDOA_{21})}{\partial x} & \frac{\partial(TDOA_{21})}{\partial y} & \frac{\partial(TDOA_{21})}{\partial z} \\ \frac{\partial(TDOA_{31})}{\partial x} & \frac{\partial(TDOA_{31})}{\partial y} & \frac{\partial(TDOA_{31})}{\partial z} \\ \vdots & \vdots & \vdots \\ \frac{\partial(TDOA_{n1})}{\partial x} & \frac{\partial(TDOA_{n1})}{\partial y} & \frac{\partial(TDOA_{n1})}{\partial z} \end{bmatrix} \quad (11)$$

where,

Ri: geometric range truth between the i-th satellite (i.e. collector) and the rescue beacon
xi, yi, zi: position of the i-th satellite

The first order differential matrix of FDOA is as follows:

$$\frac{\partial(FDOA_{i1})}{\partial x} = \left[\frac{(x - x_i) \times \{v_{x,i}(x_b - x) + v_{y,i}(y_b - y) + v_{z,i}(z_b - z)\}}{R_i^3} - \frac{v_{x,i}}{R_i}\right] - \left[\frac{(x - x_1) \times \{v_{x,1}(x_1 - x) + v_{y,1}(y_1 - y) + v_{z,1}(z_1 - z)\}}{R_1^3} - \frac{v_{x,1}}{R_1}\right] \quad (12)$$

$$H_{FDOA} = \begin{bmatrix} \frac{\partial(FDOA_{21})}{\partial x} & \frac{\partial(FDOA_{21})}{\partial y} & \frac{\partial(FDOA_{21})}{\partial z} \\ \frac{\partial(FDOA_{31})}{\partial x} & \frac{\partial(FDOA_{31})}{\partial y} & \frac{\partial(FDOA_{31})}{\partial z} \\ \vdots & \vdots & \vdots \\ \frac{\partial(FDOA_{n1})}{\partial x} & \frac{\partial(FDOA_{n1})}{\partial y} & \frac{\partial(FDOA_{n1})}{\partial z} \end{bmatrix} \quad (13)$$

By using the first-order ordinary differential equation, the H matrix is obtained and the estimated value is iteratively calculated using this measured value:

$$\delta\underline{x} = (H^T H)^{-1} H^T \cdot \delta\underline{z} \quad (14)$$

$$\underline{x}_k = \underline{x}_{k-1} + \delta\underline{x} \quad (15)$$

where,

H: $\begin{bmatrix} H_{TDOA} \\ H_{FDOA} \end{bmatrix}$
$\delta\underline{z}$: measurement residual
$\underline{x}_k$: state vector at the k-th iteration

The iterative calculation is performed until the variation of the estimated value (δx) becomes smaller than the previously defined threshold value.

3. SIMULATION STUDY

In this section, numerical simulations are performed to evaluate the performance improvement of the second generation COSPAS-SARSAT by the use of a phased array

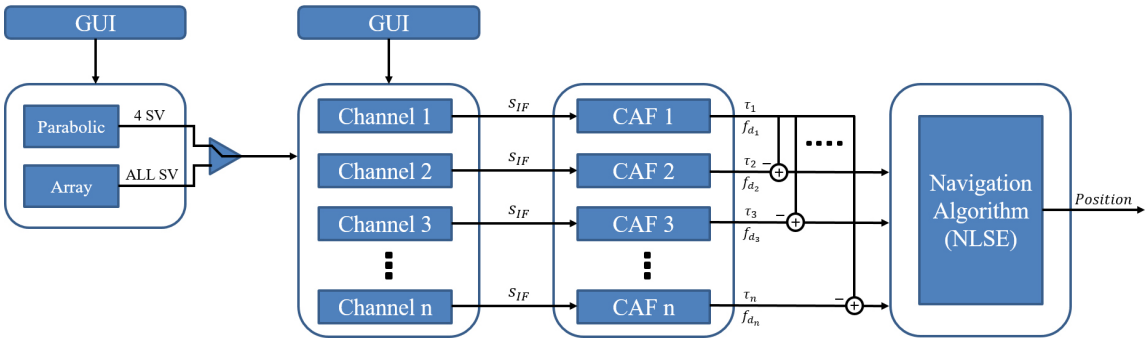

Fig. 3. Structure of COSPAS-SARSAT simulation software tool.

antenna at MEOLUT and KPS. The performance is evaluated in terms of the number of visible satellites, dilution of precision (DOP), and position estimation performance. The simulation software tool consisting of four stages, like environmental setting, signal generation, signal processing, and positioning results was built based on MATLAB.

3.1 Simulation Settings

The basic structure of the simulation software tool is shown in Fig. 3. The simulation begins with a setup of scenarios. The parameters used in the scenario can be set through the graphical user interface (GUI) and include beacon location, LUT location, Coordinated Universal Time (UTC) time, and satellite selection. When the parameters are set up, the positions of all selected satellites are calculated based on the almanacs of the selected satellites and UTC. Next, the visible satellites commonly viewed simultaneously from the beacon and LUT are selected. When a directional dish antenna is used at a MEOLUT, four visible satellites with the smallest joint dilution of precision (JDOP) (best-4 mode) are selected among all four visible satellites combinations. Conversely, a MEOLUT using a phased array antenna is assumed to use all visible satellites (all-in-view mode)

3.2 Satellite Visibility

The MEOLUT location for the visible satellites analysis is assumed to be a given point in the Korean peninsula. In the simulation, GPS, GLONASS, and Galileo are regarded as MEOSAR satellites. Satellites above an elevation angle of 18 degrees were selected as the visible satellites.

Fig. 4 shows the variation in the number of visible satellites that MEOLUT can observe for 24 h. Assuming the MEOSAR composed of GPS, GLONASS, and Galileo, an average of 20 visible satellites were observed over the Korean peninsula. When the cut-off elevation angle is

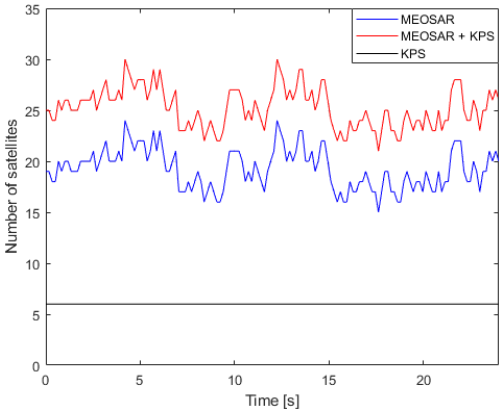

Fig. 4. MEOSAR and KPS satellite visibility.

18 degrees, KPS always observes six satellites in Korean peninsula region. Therefore, when KPS is used together with MEOSAR, the total number of visible satellites is increased by 6, and it is expected that the location estimation performance will be improved, accordingly.

3.3 JDOP

The quality of theoretical position estimation of GNSS is analyzed using DOP (Kaplan & Hegarty 2017). Unlike GNSS, COSPAS-SARSAT estimates the beacon's location using TDOA and FDOA. Therefore, the newly defined DOP for COSPAS-SARSAT is called Joint Dilution of Precision (JDOP). To define the JDOP, we first define the variance of the beacon position. Since the horizontal position is important in COSPAS-SARSAT, we consider the variance of horizontal positions ($\sigma_{horzPos}$). The equations governing the variance of the horizontal position are as follows (COSPAS-SARSAT 2018b):

$$G = \left(\frac{1}{2}\sigma_{TOA}^{-2}H_{TDOA}^{T}H_{TDOA} + \frac{1}{2}\sigma_{FOA}^{-2}H_{FDOA}^{T}H_{FDOA}\right) \quad (16)$$

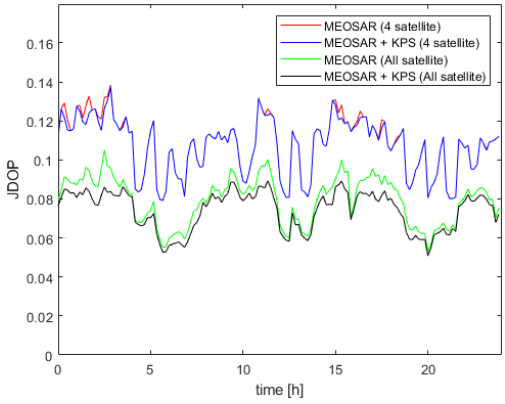

Fig. 5. JDOP for 24 hours in South Korea.

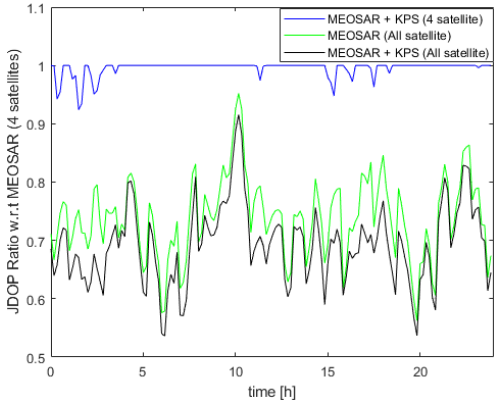

Fig. 6. JDOP ratio of MEOSAR 4 satellites to the others.

Table 1. JDOPs for various scenarios.

Scenario	JDOP [unitless]		
	min	mean	max
best-4 SVs (MEOSAR-only)	0.0792 (1)	0.1077 (1)	0.1384 (1)
best-4 SVs (MEOSAR+KPS)	0.0792 (1)	0.1071 (0.9944)	0.1373 (0.9921)
all-in-view SVs (MEOSAR-only)	0.0531 (0.6705)	0.0793 (0.7363)	0.1051 (0.7594)
all-in-view SVs (MEOSAR+KPS)	0.0509 (0.6427)	0.0742 (0.6890)	0.0892 (0.6445)

$$\sigma_{horzPos} = \sqrt{G_{11} + G_{22}} \tag{17}$$

where,

σ_{TOA}: standard deviation of TOA

σ_{FOA}: standard deviation of FOA

Gij: entry in the *i*-th row and *j*-th column of the G matrix

JDOP is defined as the relationship between the variance of the horizontal position and the measured value, that is, TOA as follows:

$$G' = \frac{1}{2}\sigma_{TOA}^{-2} G = \left(H_{TDOA}^T H_{TDOA} + \frac{\sigma_{TOA}^{-2}}{\sigma_{FOA}^{-2}} H_{FDOA}^T H_{FDOA} \right) \tag{18}$$

$$JDOP = \sqrt{G'_{11} + G'_{22}} \tag{19}$$

$$\sigma_{horzPos} = \sqrt{2}\sigma_{TOA} \times JDOP \tag{20}$$

σ_{TOA} depends on the variance of measured value and JDOP. Since JDOP depends on the geometric arrangement of satellites, it can be improved by increasing the number of visible satellites when KPS is operated together with MEOSAR. However, for a conventional dish antenna, the number of visible satellites may be limited. Thus, it is not possible to make a huge improvement in JDOP.

Fig. 5 shows the variation in the JDOP over 24 h. The red and blue lines show the JDOP calculated by the directional dish antenna (best-4) when using MEOSAR and MEOSAR+KPS, respectively. The black and green lines show the JDOP calculated by the phased array antenna (all-in-view) as indicated previously. Since the phased array antenna uses all-in-view satellites, its JDOP is always smaller than the best-4 case of the directional antenna regardless of whether KPS is operated or not. The inclusion of KPS to the satellite selection logic at the LUT improves the JDOP performance, slightly.

Fig. 6 shows the comparison of the ratios of the best-4 JDOP using only dish antenna and MEOSAR and the other scenarios. In the case of best-4 using a directional dish antenna, the number of satellites used is limited. Therefore, even if KPS is used, there is little change in JDOP, and the blue line in Fig. 6 is largely steady at a value of "1", except for certain times. Fig. 6 also shows that the all-in-view method using phased array antennas and the addition of KPS outperforms all other scenarios.

Table 1 shows the average, maximum, and minimum values of JDOP for each scenario, where the values in parenthesis represent the ratio with respect to the best-4 satellite case when MEOSAR is only used. Although KPS is used with a dish antenna, the best-4 satellites may not include any KPS satellites. Therefore, the improvement in JDOP performance is not foreseen. However, JDOP is greatly improved when a phased array antenna is used. Comparing the use of the directional dish antenna and the phased array antenna, the mean JDOP decreases to about 73% when only MEOSAR is used, and the mean JDOP decreases to about

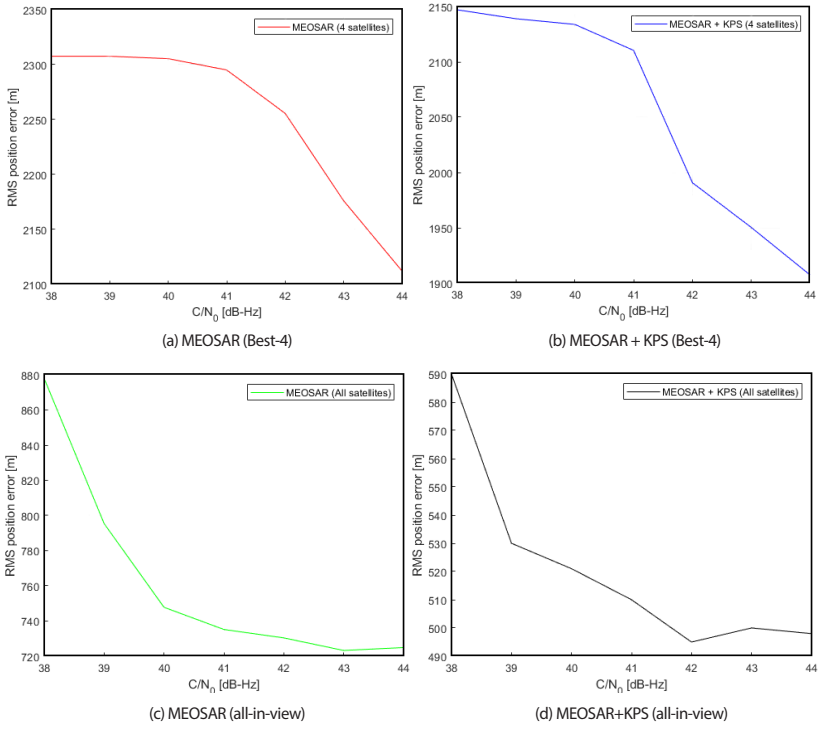

Fig. 7. RMS position errors.

68% when MEOSAR is used together with KPS.

3.4 Positioning Accuracy

The variance of the horizontal position ($\sigma_{horzPos}$) estimated in COSPAS-SARSAT is affected not only by the JDOP but also by the variance of the measured values (σ_{TOA}). Therefore, the position accuracy analysis is performed according to various C/N_0 values, which determine σ_{TOA} and JDOP. The simulation settings are as follows. To analyze the position estimation performance according to various C/N_0, we conduct 1000 simulation runs for each C/N_0. The sampling rate is set to 0.2 MHz and the simulation is performed when the change in the JDOP according to the use of KPS is greatest.

Fig. 7 shows the position error of each scenario according to C/N_0. First, in all scenarios, the position error decreases as C/N_0 increases. In Fig. 7a, we use a directional dish antenna and MEOSAR only, and has the largest position error among all the scenarios. Fig. 7b shows the position error result when KPS is added to the scenario in Fig. 7a. In scenario (a), the JDOP is about 0.1163, whereas that in scenario (b) is about 0.1156. With the addition of KPS, the JDOP as well as the position error are slightly improved.

In Fig. 7c, we use phased array antennas and MEOSAR only. Compared with Fig. 7a, the JDOP is improved as the number of used satellites increases, so that the position error is also remarkably reduced. Fig. 7d shows the position error when KPS is added to the scenario in Fig. 7c. In scenario (a), the JDOP is about 0.1163, whereas that in scenario (b) is about 0.1156. With the addition of KPS, the JDOP and the position error are slightly improved. In scenarios (c) and (d), the JDOP is about 0.952 and 0.0845, respectively. Therefore, scenario (d) has the largest position error among all the scenarios.

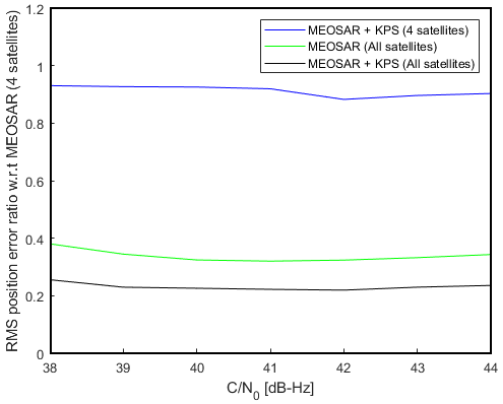

Fig. 8. Ratio of RMS position errors.

Fig. 8 compares the ratio of the position error using only the dish antenna and MEOSAR to that of the other scenarios. When using the dish antenna, we can see the improvement in position estimation performance, as shown

by the blue line in Fig. 8, for a certain time. However, when using a phased array antenna with MEOSAR only, the position estimation performance increases, as shown by the green line in Fig. 8. Specifically, the position estimation performance is the best when operating KPS with MEOSAR and using a phased array antenna.

Table 2 shows the results of position error according to C/N_0 for each scenario. When MEOLUT uses a directional dish antenna, the position error is reduced to 93% by simply operating KPS with MEOSAR. When MEOLUT uses a phased array antenna, the position error is reduced by up to 38%. If MEOLUT is operated together with KPS, the position error is reduced to 25%.

4. CONCLUSTIONS

This study aimed to evaluate the service performance of COSPAS-SARSAT provided by existing MEOSAR and planned KPS. The performance improvement was obtained by using phased array antennas at a MEOLUT in order to effectively cover all the visible satellites that were increased dramatically due to the inclusion of MEOSAR to the second generation COSPAS-SARSAT and the additional use of KPS.

The analysis was performed for the number of visible satellites, JDOP, and position estimation error according to the use of the phased-array antenna as well as the operation of KPS. When operating KPS together with MEOSAR, we can expect to see an increase in the number of visible satellites over time. When the JDOP was compared based on the increase in the number of visible satellites, there was no significant improvement in JDOP for the directional dish antenna. On the other hand, when using a phased array antenna, the average JDOP reduced to about 99% and the position error decreased to 93%.

For the comparison of the directional dish antenna and phased array antenna, we analyzed the performance of the JDOP and position estimation error. When an LUT uses the phased array antenna, the number of available satellites is increased, and the average JDOP decreases to about 69% and the position error decreases to 25%. From results, we verified the improvement of position accuracy and JDOP performance according to KPS and phased array antenna operation. It will be helpful for improve location estimation performance when COSPAS-SARSAT is operated in Korea.

ACKNOWLEDGMENTS

This work has been supported by the National GNSS Research Center program of Defense Acquisition Program Administration and Agency for Defense Development.

AUTHOR CONTRIBUTIONS

Lee, J.H. and Won, J.H. contributed to the design and implementation of the research, to the analysis of the results and to the writing of the manuscript. “Conceptualization, Lee, J.H., Lee, S. and Won, J.H.; Methodology, Lee, J.H. and Won, J.H..; Software, Lee, J.H. ; Validation: Lee, J.H. and Won, J.H.; Formal analysis, Lee, J.H.; Investigation: Lee, J.H. and Won, J.H.; Resources: Lee, J.H., Lee. S. and Won, J.H.; Data curation, Lee, J.H.; Writing-original draft Preparation: Lee, J.H.; Writing-review and editing: Lee, J.H. and Won, J.H.; Visualization, Lee, J.H.; Supervision, Won, J.H.; Project administration, Won, J.H.; Funding Acquisition, Lee, S.; This manuscript has not been published or presented elsewhere in part or in entirety, and is not under consideration by another journal. There are no conflicts of interest to declare.

CONFLICTS OF INTEREST

The authors declare no conflict of interest.

REFERENCES

COSPAS-SARSAT 2018a, COSPAS-SARSAT System, 11 October 2018. [Online] Available: https://cospas-sarsat.int/en/

COSPAS-SARSAT 2018b, COSPAS-SARSAT MEOLUT Performance Specification and Design Guidelines, C/S T.019 Issue 2 - Revision 2, 2018. [Online] Available: https://cospas-sarsat. int/images/stories/SystemDocs/Current/CS-T019-JUN-27-2018.pdf

COSPAS-SARSAT 2018c, COSPAS-SARSAT 406 MHz MEOSAR Implementation Plan, C/S R.012 Issue 1 – Revision 12 [Online]. Available: https://cospas-sarsat.int/images/stories/SystemDocs/Current/CS-R012-FEB-2018.pdf

COSPAS-SARSAT 2018d, Specification for Second-Generation COSPAS-SARSAT 406-MHz Distress Beacon, C/S T.018 Issue 1 – Revision 2. [Online] Available: https://cospas-sarsat. int/images/stories/SystemDocs/Current/CS-T018-JUN-27-2018.pdf

GPS World 2018, Korea will Launch its Own Satellite Positioning System, GPS World, 5 Feb. 2018. [Online] Available: https://www.gpsworld.com/korea-will-

launch-its-own-satellite-positioning-system/
Hartwell, G. D. 2005, Improved geo-spatial resolution using a modified approach to the complex ambiguity function (CAF), Master's Dissertation, Naval Postgraduate School, California, CA. http://hdl.handle.net/10945/2033
Jeong, I, Lee, S., & Ahn, W.-G. 2019, Implementation of the Modeling and Simulation Software of Search and Rescue System based Korea Navigation Satellite System, E3S Web Conf. Vol. 94, 2019. https://doi.org/10.1051/e3sconf/20199401025
Kaplan, E. D. & Hegarty, C. J. 2017, Understanding GPS/GNSS: Principles and Applications, 3rd ed (Massachusetts: Artech House)
Lee, J. H., Jeong, I., & Won, J. H. 2018, BASS Algorithm for Enhanced Position Estimation of MEOSAR COSPAS-SARSAT Receivers, Proceedings of the 2018 International Technical Meeting of The Institute of Navigation, Reston, Virginia, January 2018, pp.292-300.
Martin, P., Calmettes, T., Gregoire, Y., Reche, M., Chatain, C., et al. 2018, The COSPAS-SARSAT MEOSAR System: A Solution to Support ICAO GADSS Autonomous Distress Tracking Recommendation, Inside GNSS, 12 June 2018. [Online] Available: http://insidegnss.com/THE-COSPAS-SARSAT-MEOSAR-SYSTEM/
Paiement, R., Caron, M., & Tang, X. 2008, Dilution of Precision Factor in Medium Earth Orbit Search and Rescue Systems, Proceedings of the International Technical Meeting of the Satellite Division of the Institute of Navigation: ION-GNSS 2008, 16-19 September, Savannah, GA, USA, 2008, pp.2700-2705
Tsui, Y. B. J. 2005, Fundamentals of Global Positioning System Receivers: A Software Approach, 2nd ed. (New York: John Wiley & Sons)

Jung-Hoon Lee received the master's degree in Autonomous Navigation Laboratory of Department of Electrical Engineering at Inha University, Incheon, South Korea in 2019. He is currently working with the Network Business Global Technology Service Team of Samsung Electronics, Suwon, South Korea. His research interests include software receiver and navigation applications.

Sanguk Lee received the Ph. D. degree in Department of Aerospace Engineering from Auburn University, Alabama, USA, in 1994. He joined Electronics & Telecommunication Research Institute (ETRI) and has been working now. He had worked on satellite simulator of satellite ground control systems for KOREASAT, KOMPSAT 1 & 2 and COMS in his first half and he has been working GNSS related research such as SW based GNSS (GPS&Galileo), GNSS Infrastructure, GPS Interference Detection Mitigation & Localization. in his second half at ETRI. Currently, his research interests are Cloud GNSS, GNSS Anti-jamming & Spoofing, Alternative Navigation, SSV, GNSS-R, Precise Positioning and so on.

Jong-Hoon Won received the Ph.D. degree in the Department of Control Engineering from Ajou University, Korea, in 2005. After then, he had worked with the Institute of Space Application at University Federal Armed Forces (UFAF) Munich, Germany. He was nominated as Head of GNSS Laboratory in 2011 at the same institute, and involved in lectures on advanced receiver technology at Technical University of Munich (TUM) since 2009. He is currently an associate professor of the Department of Electrical Engineering at Inha University. His research interests include GNSS signal design, receiver, navigation, target tracking systems and self-driving cars.